Journal of Computational Physics **153,** 418–436 (1999)
Article ID jcph.1999.6284, available online at http://www.idealibrary.com on IDEAL®

Open Boundary Conditions for Lagrangian Geophysical Fluid Dynamics

A. F. Bennett* and B. S. Chua†

College of Oceanic and Atmospheric Sciences, Oregon State University, Corvallis, Oregon
E-mail: *bennett@oce.orst.edu; †chua@oce.orst.edu

Received December 21, 1998; revised April 26, 1999

Initial-boundary-value problems for the *hydrostatic primitive equations* of meteorology and oceanography are ill-posed if the boundaries are open and fixed in space (Oliger and Sundström, 1978). It is shown here with theory and computation that the same problems are well-posed if the open boundaries are *comoving*, that is, if they move with the fluid particles. Comoving or Lagrangian coordinates are then particularly convenient. These findings will expedite the variational assimilation of Lagrangian data. © 1999 Academic Press

Key Words: open boundaries; Lagrangian coordinates; well-posedness.

1. INTRODUCTION

Open boundary conditions for geophysical fluid dynamics in Eulerian domains lead almost inevitably to ill-posed mixed initial-boundary-value problems [1]. By "geophysical" we mean the so-called *hydrostatic primitive equations* [2]. These make only minor geometrical approximations to the laws of conservation of horizontal momentum, but assume that the vertical pressure gradient is in exact hydrostatic balance with the buoyancy force per unit volume. The ill-posedness arises whenever the particle speeds lie within the range of the phase speeds of the hydrostatic internal gravity waves: the flow is then subcritical with respect to the graver, faster modes and supercritical with respect to the higher, slower modes. Thus boundary conditions that are not applied mode-by-mode must either overdetermine some modes or underdetermine the others. In most numerical models, the boundary conditions are applied pointwise in the vertical, and so ill-posedness is manifest [3–6]. The difficulty arises both in "level" models for which the vertical coordinate is depth and also in "layer" models for which the "vertical" coordinate is a thermodynamic state variable such as density: see Section 9.3 of [7].

The difficulty is removed by a Galilean transformation to the reference frame of the fluid particles. Then information about the flow divergence propagates at the gravity wave speed, while information about the vorticity does not radiate as the latter is conserved on

0021-9991/99 $30.00
Copyright © 1999 by Academic Press
All rights of reproduction in any form reserved.

fluid particles. All modes are effectively subcritical, so the number of boundary conditions required to determine the inward-propagating signals is the same for all modes. The implication is that if the boundary moves with the fluid particles, or is *comoving*, then there is no difficulty in choosing the right number of boundary conditions in order to obtain a well-posed mixed initial-boundary-value problem. The effectiveness of these boundary conditions as *radiation* conditions is a separate issue. It is emphasized that as all modes are to be subjected to the same number and type of boundary conditions, these conditions may be applied pointwise in the vertical. That is, no modal expansion is necessary. However, the comoving reference frame is in general depth dependent and thus will lead to distortion of initially rectilinear domains.

The structure of this paper is as follows. The difficulties with boundary conditions at Eulerian or fixed open boundaries are reviewed in Section 2, using the classical energy arguments [1]. It suffices to use just the shallow-water equations in this analysis. The same energy arguments applied to comoving boundaries indicate no difficulties. The Lagrangian form of the equations is reviewed in Section 3, along with the Weber vorticity integral. The equations are linearized, and manipulated to reveal the linearized dynamics of the divergent motion and the rotational motion. This permits ready identification of open boundary conditions that yield well-posed problems. Radiation conditions are mentioned briefly in Section 4. Computational evidence in support of the linearized analysis is presented in Section 5, along with tests of a simple radiation condition. Implications for modeling and data assimilation are discussed in Section 6.

2. ENERGY ARGUMENTS

In plane Eulerian coordinates $\mathbf{x} = (x, y)$, the shallow-water equations are

$$\frac{\partial \mathbf{u}}{\partial t} + \mathbf{u} \cdot \boldsymbol{\nabla}\mathbf{u} + f\hat{\mathbf{k}} \times \mathbf{u} = -g\boldsymbol{\nabla}h + \mathbf{F}, \tag{2.1}$$

$$\frac{\partial h}{\partial t} + \boldsymbol{\nabla} \cdot (h\mathbf{u}) = 0, \tag{2.2}$$

where t is time, $\mathbf{u} = \mathbf{u}(\mathbf{x}, t)$ is the depth-independent plane velocity field, $\hat{\mathbf{k}}$ is a unit vector normal to the plane, $h = h(\mathbf{x}, t)$ is the water depth over a flat bottom, g is the gravitational acceleration, and $\mathbf{F} = \mathbf{F}(\mathbf{x}, t)$ is body force per unit mass. The Coriolis parameter f is assumed to be a linear function of y—$f = f(y) = f_0 + \beta y$—thus (2.1) represents dynamics on the β-plane [8]. Equations (2.1) and (2.2) are assumed to hold in some simply connected, bounded plane domain $\mathcal{D}$ with piecewise smooth boundary $\mathcal{B}$; see Fig. 1. Suitable initial conditions for (2.1) and (2.2) are

$$\mathbf{u}(\mathbf{x}, 0) = \mathbf{u}_I(\mathbf{x}), \qquad h(\mathbf{x}, 0) = h_I(\mathbf{x})\,. \tag{2.3}$$

Let $\mathbf{u}^{(1)}, h^{(1)}$ and $\mathbf{u}^{(2)}, h^{(2)}$ be two solutions for the same forcing $\mathbf{F}$ and initial values $\mathbf{u}_I, h_I$ and let $\mathbf{U} = \mathbf{u}^{(1)} - \mathbf{u}^{(2)}$, $H = h^{(1)} - h^{(2)}$ be the difference fields. Oliger and Sundström [1] have shown that

$$\begin{aligned}\frac{\partial}{\partial t}\left(h^{(1)}K + P\right) &+ \boldsymbol{\nabla} \cdot \left[\mathbf{u}^{(1)}\left(h^{(1)}K + P\right) + gh^{(1)}H\mathbf{U}\right] \\ &= gH\mathbf{U} \cdot \boldsymbol{\nabla}h^{(1)} - gH\mathbf{U} \cdot \boldsymbol{\nabla}h^{(2)} - gH^2\boldsymbol{\nabla} \cdot \mathbf{u}^{(2)} \\ &\quad + P\boldsymbol{\nabla} \cdot \mathbf{u}^{(1)} - h^{(1)}\mathbf{U} \cdot (\mathbf{U} \cdot \boldsymbol{\nabla})\mathbf{u}^{(2)},\end{aligned} \tag{2.4}$$

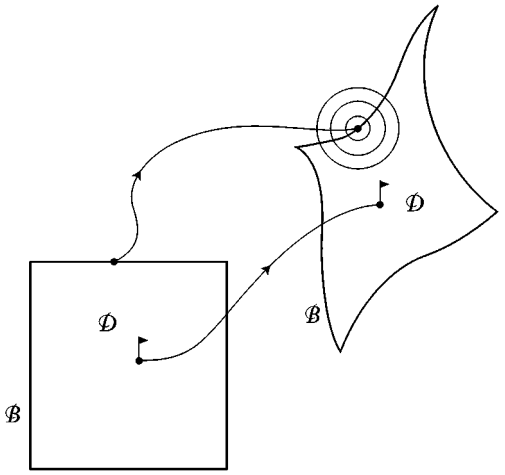

FIG. 1. A comoving domain $\mathcal{D}$ with boundary $\mathcal{B}$. Vorticity is conserved along particle paths; divergence radiates toward and away from particle paths via gravity waves.

where

$$K = \frac{1}{2}\mathbf{U}\cdot\mathbf{U}, \qquad P = \frac{1}{2}gH^2 \tag{2.5}$$

are respectively the kinetic and potential energies of the difference fields $\mathbf{U}$, H. It follows from (2.4) that

$$\frac{dE}{dt} + A \le BE, \tag{2.6}$$

where

$$E = E(t) \equiv \iint_{\mathcal{D}} \left(h^{(1)}K + P\right) d\mathbf{x} \tag{2.7}$$

$$A = A(t) \equiv \int_{\mathcal{B}} \left\{\mathbf{u}^{(1)}\cdot\hat{\mathbf{n}}\left(h^{(1)}K + P\right) + gh^{(1)}H\mathbf{U}\cdot\hat{\mathbf{n}}\right\} ds \tag{2.8}$$

$$B \equiv \left(\frac{11}{2}\right) \max_{i,\mathbf{x},t} \left\{\left|\boldsymbol{\nabla}\cdot\mathbf{u}^{(i)}\right|, \left(g/h^{(i)}\right)^{1/2}\left|\boldsymbol{\nabla}h^{(i)}\right|\right\} \tag{2.9}$$

and $\hat{\mathbf{n}}$ is the outward unit normal on $\mathcal{B}$. Integrating (2.6) yields

$$E(t) \le E(0) - \int_0^t e^{B(t-r)}A(r)\,dr. \tag{2.10}$$

Note that the inverse time scale B is independent of the time r.

Now $E(0) = 0$, since the two solutions satisfy the same initial condition. We next verify that $E(t) \ge 0$, by showing that $h^{(1)} \ge 0$. A formal solution for $h^{(1)}$ may be obtained by integrating (2.2) along a particle path. Let $\mathbf{X}(\mathbf{x}, t\,|\,r)$ be the position at time r of a fluid

particle that passes through $\mathbf{x}$ at time t [9]. Then

$$\frac{\partial \mathbf{X}}{\partial r} = \mathbf{U}(\mathbf{X}, r) \tag{2.11}$$

and

$$\mathbf{X}(\mathbf{x}, t \mid t) = \mathbf{x}. \tag{2.12}$$

Then the formal solution of (2.2) is

$$h(\mathbf{x}, t) = h_I(\mathbf{X}(\mathbf{x}, t \mid 0)) \exp\left\{ -\int_0^t \delta(\mathbf{x}, t \mid r)\, dr \right\}, \tag{2.13}$$

where

$$\delta(\mathbf{x}, t \mid r) = (\nabla \cdot \mathbf{u})(\mathbf{X}(\mathbf{x}, t \mid r), r) \tag{2.14}$$

is the flow divergence at the particle at $(\mathbf{X}, r)$. So if $h_I \geq 0$ and if δ is integrable with respect to r, then $h(\mathbf{x}, t) \geq 0$. Hence $E(t) \geq 0$.

Returning to (2.10), it is now clear that any boundary condition which ensures $A \geq 0$ also ensures that $E(t) \equiv 0$, that is, the mixed-initial-boundary value problem has a unique solution.

The integrand in (2.8) is a 3×3 quadratic form over $(\mathbf{U}, H)$. Its eigenvalues and eigenvectors determine the appropriate number and type of *linear* boundary conditions for uniqueness of solutions. There are four cases.

(i) Subcritical outflow $[0 < \mathbf{u}^{(1)} \cdot \hat{\mathbf{n}} < (gh^{(1)})^{1/2}]$:

$$\text{one boundary condition:} \qquad \mathbf{U} \cdot \mathbf{n} = \left(g/h^{(1)}\right)^{1/2} H. \tag{2.15a}$$

(ii) Supercritical outflow $[0 < (g/h^{(1)})^{1/2} < \mathbf{u}^{(1)} \cdot \hat{\mathbf{n}}]$:

$$\text{no boundary conditions.} \tag{2.15b}$$

(iii) Subcritical inflow $[-(g/h^{(1)})^{1/2} < \mathbf{u}^{(1)} \cdot \hat{\mathbf{n}} < 0]$:

$$\text{two boundary conditions:} \qquad \mathbf{U} \cdot \hat{\mathbf{n}} = -\left(g/h^{(1)}\right)^{1/2} H, \qquad \mathbf{U} \cdot \hat{\mathbf{s}} = 0; \tag{2.15c}$$

where $\hat{\mathbf{s}}$ is the unit tangent on $\mathcal{B}$.

(iv) Supercritical inflow $[\mathbf{u}^{(1)} \cdot \hat{\mathbf{n}} < -(gh^{(1)})^{1/2}]$:

$$\text{three boundary conditions:} \qquad \mathbf{U} \cdot \hat{\mathbf{n}} = \mathbf{U} \cdot \hat{\mathbf{s}} = H = 0. \tag{2.15d}$$

The above conditions are expressed in terms of the difference fields $\mathbf{U}$, H. As applied to (2.1), (2.2), and (2.3), case (i), for example, would be

$$[0 < \mathbf{u} \cdot \hat{\mathbf{n}} < (gh)^{1/2}]; \qquad \mathbf{u} \cdot \hat{\mathbf{n}} = (g/h)^{1/2} h + R, \tag{2.16}$$

where $R = R(s, t)$ is some boundary forcing.

Notes. (i) The initial condition (2.3) and boundary conditions (2.15) are linear. The dynamics (2.1), (2.2) are nonlinear.

(ii) The above uniqueness proof is readily modified to show also that the solution, should it exist, depends continuously upon the initial values, body forcing, and boundary forcing. It is not possible to prove existence of a smooth solution for an arbitrarily long time interval, given even smooth initial values, etc., owing to the tendency to form bores or hydraulic jumps. That is, a complete proof of well-posedness is not possible, so we shall use "well-posedness" in the restricted sense of uniqueness (and continuous dependence upon data).

(iii) Rotation does not explicitly influence the energy budget (2.4), nor does it influence the choices of open boundary conditions in (2.15).

The assumption of an Eulerian, or spatially and temporally fixed open boundary $\mathcal{B}$, is essential to the derivation of the energy inequality (2.6). Now suppose $\mathcal{B}$ is Lagrangian, consisting of a set of fluid particles of fixed identity. That is, suppose $\mathcal{B}$ is defined by

$$\theta(\mathbf{x}, t) = \theta_0 \tag{2.17}$$

for some smooth function θ and some constant θ_0, where θ satisfies

$$\frac{\partial \theta}{\partial t} + \mathbf{u} \cdot \boldsymbol{\nabla} \theta = 0 \tag{2.18}$$

on $\mathcal{B}$. It may be shown that, for such a comoving boundary, θ must be of the form

$$\theta(\mathbf{x}, t) = \theta_I(\mathbf{X}(\mathbf{x}, t \mid 0)), \tag{2.19}$$

where

$$\theta_I(\mathbf{x}) = \theta(\mathbf{x}, 0). \tag{2.20}$$

Integrating (2.4) over the comoving domain $\mathcal{D}$ interior to $\mathcal{B}$ yields

$$\frac{dE}{dt} + C \leq BE, \tag{2.21}$$

where E and B are defined as before—see (2.7), (2.9)—while

$$C = C(t) \equiv \int_{\mathcal{B}} gh^{(1)} H \mathbf{U} \cdot \hat{\mathbf{n}} \, ds. \tag{2.22}$$

The fluid works on the pressure field at the boundary, but there is no advective flux of mechanical energy across the boundary: compare (2.22) with (2.8). Integrating (2.21) yields

$$E(t) = E(0) - \int_0^t e^{B(t-r)} C(r) \, dr. \tag{2.23}$$

Uniqueness follows from any *one* boundary condition that ensures $C \geq 0$, such as

(i) $$H = 0, \tag{2.24a}$$

(ii) $$\mathbf{U} \cdot \hat{\mathbf{n}} = 0, \tag{2.24b}$$

or

(iii) $$\mathbf{U}\cdot\hat{\mathbf{n}} = k\left(g/h^{(1)}\right)^{1/2} H, \tag{2.24c}$$

where $k \geq 0$. The scale factor is included in (2.24c) for dimensional homogeneity. The criticality of the flow at the boundary is not an issue. Indeed, in the comoving reference frame the effective local Froude number is identically zero. Information can only cross the comoving boundary by gravity-wave propagation.

What the preceding analysis does not make clear is the number of boundary conditions needed to specify the comoving boundary $\mathcal{B}$. Must both components of $\mathbf{u}$ be provided on $\mathcal{B}$? Specifying the boundary function $\theta(\mathbf{x}, t)$ determines the normal component $\mathbf{u}\cdot\hat{\mathbf{n}}$, via the comoving condition (2.18). Does that suffice? Is it necessary to specify $\mathbf{u}\cdot\hat{\mathbf{s}}$ or h as well? Is it even permissible to specify $\theta(\mathbf{x}, t)$?

3. LAGRANGIAN COORDINATES

A linearized analysis of the Lagrangian form of the equations of motion reveals the correct number of open boundary conditions for the shallow-water equations.

Let $\mathbf{a} = (a, b)$ be the initial Cartesian coordinates of a fluid particle, and let $\mathbf{X} = (X, Y) = \mathbf{X}(\mathbf{a}, t)$ be the Cartesian coordinates of the particle time $t \geq 0$. In terms of the more general notation used in the previous section, $\mathbf{X}(\mathbf{a}, t) = \mathbf{X}(\mathbf{a}, 0 \mid t)$. The conservation of momentum (2.1) is expressed as

$$\frac{\partial^2 X}{\partial t^2} = -gJ^{-1}\left\{\frac{\partial h}{\partial a}\frac{\partial Y}{\partial b} - \frac{\partial h}{\partial b}\frac{\partial Y}{\partial a}\right\} \tag{3.1}$$

$$\frac{\partial^2 Y}{\partial t^2} = -gJ^{-1}\left\{\frac{\partial X}{\partial a}\frac{\partial h}{\partial b} - \frac{\partial X}{\partial b}\frac{\partial h}{\partial a}\right\}, \tag{3.2}$$

where J is the Jacobian

$$J \equiv \frac{\partial(X, Y)}{\partial(a, b)} \equiv \frac{\partial X}{\partial a}\frac{\partial Y}{\partial b} - \frac{\partial X}{\partial b}\frac{\partial Y}{\partial a}. \tag{3.3}$$

The partial derivatives with respect to time refer to fixed values of (a, b). Rotation and the body force $\mathbf{F}$ have been neglected as they do not affect our conclusions.

Conservation of volume is expressed as

$$\frac{\partial(hJ)}{\partial t} = 0. \tag{3.4}$$

Certainly we must specify initial conditions for $\mathbf{X}$, $\mathbf{U} \equiv \frac{\partial \mathbf{X}}{\partial t}$, and h:

$$\mathbf{X}(\mathbf{a}, 0) = \mathbf{a}, \tag{3.5}$$

$$\mathbf{U}(\mathbf{a}, 0) \equiv \frac{\partial \mathbf{X}}{\partial t}(\mathbf{a}, 0) = \mathbf{U}_I(\mathbf{a}), \tag{3.6}$$

$$h(\mathbf{a}, 0) = h_I(\mathbf{a}). \tag{3.7}$$

Rearranging (3.4) as

$$\frac{\partial h}{\partial t} = -\frac{h}{J}\frac{\partial J}{\partial t}, \tag{3.8}$$

differentiating with respect to t, using (3.1)–(3.3), and retaining only leading order terms yields

$$\frac{\partial^2 h}{\partial t^2} = \frac{gh}{J^2}\left\{\left[\left(\frac{\partial X}{\partial b}\right)^2 + \left(\frac{\partial Y}{\partial b}\right)^2\right]\frac{\partial^2 h}{\partial a^2} - 2\left(\frac{\partial X}{\partial a}\frac{\partial X}{\partial b} + \frac{\partial Y}{\partial a}\frac{\partial Y}{\partial b}\right)\frac{\partial^2 h}{\partial a \partial b} + \left[\left(\frac{\partial X}{\partial a}\right)^2 + \left(\frac{\partial Y}{\partial a}\right)^2\right]\frac{\partial^2 h}{\partial b^2}\right\} + \cdots \tag{3.9}$$

Assume that $\partial X/\partial a$, etc., are given. Then (3.9) is a linear equation for h. Examining the discriminant of the second order operator on the right-hand side reveals that the equation is hyperbolic, unless the Jacobian J vanishes. This is the fundamental pathology for Lagrangian coordinates, and so need not be dwelled upon here. A suitable boundary condition for (3.9) is

$$\text{(Dirichlet)} \qquad h = 0, \tag{3.10a}$$

$$\text{(Neumann)} \qquad \hat{\mathbf{n}} \cdot \boldsymbol{\nabla} h = 0, \tag{3.10b}$$

or

$$\text{(Robin)} \qquad \alpha h + \hat{\mathbf{n}} \cdot \boldsymbol{\nabla} h = 0 \tag{3.10c}$$

for $\alpha \geq 0$. The surface height h having been determined, the particle displacements (X, Y) may be found. First, we need the two-dimensional form of the Weber vorticity-conservation law [10], which may be derived from (3.1) and (3.2):

$$\frac{\partial}{\partial t}\left[\frac{\partial^2 X}{\partial t \partial a}\frac{\partial X}{\partial b} - \frac{\partial^2 X}{\partial t \partial b}\frac{\partial X}{\partial a} + \frac{\partial^2 Y}{\partial t \partial a}\frac{\partial Y}{\partial b} - \frac{\partial^2 Y}{\partial t \partial b}\frac{\partial Y}{\partial a}\right] = 0. \tag{3.11}$$

Next, let $\bar{\mathbf{X}}$, $\bar{h}$ be time-dependent solutions of (3.1)–(3.7), and let $\mathbf{X}$, h be nearby solutions

$$X = \bar{X} + \xi, \qquad Y = \bar{Y} + \eta, \qquad h = \bar{h} + \chi, \tag{3.12}$$

where

$$|\boldsymbol{\xi}| = |(\xi, \eta)| \leq |\bar{\mathbf{X}}|, \qquad |\chi| \leq \bar{h}. \tag{3.13}$$

The linearized form of (3.3) is

$$j \equiv B\xi + C\eta, \tag{3.14}$$

where

$$B \equiv \frac{\partial \bar{Y}}{\partial b}\frac{\partial}{\partial a} - \frac{\partial \bar{Y}}{\partial a}\frac{\partial}{\partial b}, \qquad C \equiv \frac{\partial \bar{X}}{\partial a}\frac{\partial}{\partial b} - \frac{\partial \bar{X}}{\partial b}\frac{\partial}{\partial a}. \tag{3.15}$$

After one integration in time, linearization of (3.4) and (3.11) yields

$$j\bar{h} + \bar{J}\chi = 0, \tag{3.16}$$

$$\frac{\partial}{\partial t}\left[B\frac{\partial \eta}{\partial t} - C\frac{\partial \xi}{\partial t} - \frac{\partial B}{\partial t}\eta + \frac{\partial C}{\partial t}\xi\right] = 0. \tag{3.17}$$

Combining (3.14) and (3.16),

$$B\xi + C\eta = -\bar{\bar{J}}\,\bar{\bar{h}}^{-1}\chi = (\text{known}). \tag{3.18}$$

Integrating (3.17) in time and rearranging yields

$$\frac{\partial}{\partial t}[B\eta - C\xi] - 2\frac{\partial B}{\partial t}\eta + 2\frac{\partial C}{\partial t}\xi = (\text{initial values}). \tag{3.19}$$

Stepping (3.19) forward in time yields

$$B\eta - C\xi = (\text{known}). \tag{3.20}$$

Decoupling (3.18) and (3.20) yields, to leading order,

$$(B^2 + C^2)(\xi, \eta) = (\text{known, known}). \tag{3.21}$$

The elliptic equation (3.21) for, say, ξ requires only a Dirichlet, Neumann, or Robin boundary condition as in (3.10). Then ξ would be determined throughout $\mathcal{B}$, and the boundary values of both the normal *and* tangential derivatives of η could be inferred from (3.18) and (3.20). However these would be compatible boundary conditions for the elliptic problem (3.21) for η, and so η would be well-determined throughout $\mathcal{B}$.

In summary, suitable linear open boundary conditions for the nonlinear shallow water equations are

(i) specified surface height h and (ii) specified "normal" particle displacement $\mathbf{X}\cdot\hat{\mathbf{n}}$. (3.22)

In particular, the comoving boundary is then determined. It may be more convenient, when expressing the comoving domain in Eulerian coordinates, to specify h and the normal velocity:

$$\mathbf{U}\cdot\hat{\mathbf{n}} = \frac{\partial \mathbf{X}}{\partial t}\cdot\hat{\mathbf{n}}. \tag{3.23}$$

4. RADIATION BOUNDARY CONDITIONS

(a) *Eulerian Coordinates, Fixed Boundary*

The integral A defined by (2.8) is the rate of advection of total mechanical energy outward across the boundary $\mathcal{B}$, plus the rate of work by the fluid in the interior of $\mathcal{D}$ against the pressure at $\mathcal{B}$. Thus A encapsulates the interaction between the fluid in $\mathcal{D}$ and the outside world. If the chosen boundary conditions ensure that A is nonnegative, then regardless of their dynamical appropriateness, such conditions also ensure that the mathematical mixed, initial-boundary-value problem within $\mathcal{D}$ is well-posed. The choices listed as (i)–(iv) in (2.15) do ensure $A \geq 0$, but they are not the only choices. For compactness, let us introduce a dimensionally homogeneous three-vector field

$$\mathbf{W}(\mathbf{x}, t) = \begin{pmatrix} \mathbf{U}(\mathbf{x}, t) \\ \left(g/h^{(1)}\right)^{\frac{1}{2}} H(\mathbf{x}, t) \end{pmatrix}. \tag{4.1}$$

Then (2.8) becomes

$$A = \int_{\mathcal{D}} Q \, ds, \tag{4.2}$$

where the integrand Q is a quadratic form:

$$Q(s) = \mathbf{W}(s)^T \mathbf{M}(s) \mathbf{W}(s). \tag{4.3}$$

The matrix $\mathbf{M}$ in (4.3) has dimension 3×3 and is symmetric. Only the boundary coordinate s is displayed in (4.3). Diagonalizing $\mathbf{M}$ as

$$\mathbf{M} = \mathbf{Z}\mathbf{L}\mathbf{Z}^T, \tag{4.4}$$

where $\mathbf{Z}$ is orthonormal and $\mathbf{L} = \text{diag}(\lambda_1, \lambda_2, \lambda_3)$, leads to

$$Q = \mathbf{S}^T \mathbf{L} \mathbf{S}, \tag{4.5}$$

where

$$\mathbf{S} = \mathbf{Z}^T \mathbf{W}$$

is the vector of projections of the three-vector $\mathbf{W}$ upon the eigenvectors of $\mathbf{M}$. In detail, (4.5) is

$$Q = \sum_{n=1}^{3} \lambda_n S_n^2. \tag{4.6}$$

Consider case (iii): subcritical inflow. Then $\lambda_1 > 0 > \lambda_2 > \lambda_3$. Two boundary conditions are needed, such as $S_2 = S_3 = 0$, which unravel as (2.15c). More generally,

$$S_3 = 0 \tag{4.7a}$$

$$S_1 = kS_2 \tag{4.7b}$$

suffice, provided

$$k^2 \geq -\lambda_2/\lambda_1. \tag{4.8}$$

Otherwise k may be any real function of the boundary coordinate s.

Suppose now that $\mathcal{B}$ is the entire x-axis (thus $s = x$), and ignore the dependence of $\mathbf{M}$ and hence $\mathbf{L}$ upon s. Then

$$A = \int_{-\infty}^{\infty} \mathbf{S}^T \mathbf{L} \mathbf{S} \, dx = 2\pi \int_{-\infty}^{\infty} \hat{\mathbf{S}}^* \mathbf{L} \hat{\mathbf{S}} \, d\kappa, \tag{4.9}$$

where $\hat{\mathbf{S}}(\kappa)$ is the Fourier transform of $\mathbf{S}(x)$,

$$\hat{\mathbf{S}}(\kappa) = \int_{-\infty}^{\infty} e^{i\kappa x} \mathbf{S}(x) \, dx, \tag{4.10}$$

and $\hat{\mathbf{S}}^*$ is the conjugate transpose of $\hat{\mathbf{S}}$. It may now be seen that suitable boundary conditions are

$$\hat{S}_3 = 0, \tag{4.11a}$$

$$\hat{S}_1 = \hat{k}\hat{S}_2, \tag{4.11b}$$

provided $\hat{k} = \hat{k}(\kappa)$ is real, and

$$\hat{k}^2 \geq -\lambda_2/\lambda_1. \tag{4.12}$$

Otherwise $\hat{k}$ is any function of κ. The wavenumber-local condition (4.11b) is equivalent to the spatially nonlocal condition

$$S_1(x) = (2\pi) \int_{-\infty}^{\infty} k(x') S_2(x - x')\, dx'. \tag{4.13}$$

The advantage of such a condition is that it may be possible to choose k such that (4.13) is identically satisfied by motions initialized or forced within $\mathcal{D}$. Then (4.13) would in no way inhibit signals from escaping $\mathcal{D}$, but would still specify any incoming signals. That would be an ideal condition for an open or unphysical boundary [11]. Implementation of nonlocal conditions is usually impractical, and local approximations have been devised [12].

(b) *Eulerian Coordinates, Comoving Domain*

It is immediately evident from (2.24c) that, provided boundary variations of $h^{(1)}$ are ignored, a nonlocal condition of the form

$$U(x) = \left(g/h^{(1)}\right)^{1/2} \int_{-\infty}^{\infty} k(x') H(x - x')\, dx', \tag{4.14}$$

for any $k = k(x) > 0$, ensures uniqueness. Operator-splitting forms for k do exist. These forms make (4.14) an identity for signals from within $\mathcal{D}$.

(c) *Lagrangian Coordinates, Comoving Domain*

The simplest approach is to derive the following energy budget from the unperturbed equations (3.1)–(3.4)

$$\frac{d}{dt}\frac{1}{2}\iint_{\mathcal{D}} \left\{ h\left(X_t^2 + Y_t^2\right) + \frac{1}{2} g h^2 \right\} J\, da\, db = -\int_{\mathcal{B}} \mathbf{F} \cdot \hat{\mathbf{n}}\, dp, \tag{4.15}$$

where p is path length along $\mathcal{B}$ in the labelling (a, b)-space, with $\mathcal{D}$ on the left as p increases, while $\mathbf{F}$ is the directed rate of working:

$$\mathbf{F} = \frac{1}{2} g h^2 (X_t Y_t - Y_t X_b, Y_t X_a - X_t Y_a). \tag{4.16}$$

If $\mathcal{B}$ is the locus of points

$$\mathbf{a} = \mathbf{A}(p) = (A(p), B(p)), \tag{4.17}$$

then the unit normal to $\mathcal{B}$ is

$$\hat{\mathbf{n}} = (B'(p), -A'(p))|\mathbf{A}'(p)|^{-1}, \tag{4.18}$$

and

$$\int_{\mathcal{B}} \mathbf{F} \cdot \hat{\mathbf{n}}\, dp = \int_{\mathcal{B}} \frac{1}{2} g h^2 \mathbf{X}_t \cdot \hat{\mathbf{n}}\, dp. \tag{4.19}$$

There will be a *loss* of energy, from $\mathcal{D}$, across $\mathcal{B}$ so long as the integrand in (4.19) is *positive*; see (4.15). As an example of a suitably "lossy" boundary condition, consider

$$\mathbf{X}_t \cdot \hat{\mathbf{n}} = k(g/h)^{1/2} h \tag{4.20}$$

for any $k \geq 0$. Recall that h does not change its sign over time, provided the flow divergence is integrable along particle paths. The perturbation form of (4.20) is, in the notation (3.12),

$$\chi = k^{-1}(g/\bar{h})^{-1/2} \boldsymbol{\xi}_t \cdot \hat{\mathbf{n}}. \tag{4.21}$$

The condition (4.21) may be uncoupled after much algebra, but direct numerical implementation of (4.21) (or (4.20)) is straightforward while $\boldsymbol{\xi}$ (or $\mathbf{X}$) is being time-stepped.

5. DEMONSTRATIONS

The theoretical arguments in Section 3 leading to the boundary conditions (3.22) are supported by a simple numerical demonstration. It involves an outer and an inner domain. The outer is a periodic channel, and the inner is a half-wavelength section of the channel; see Fig. 2. Notice that the coordinates are Lagrangian a and b (the initial Cartesian coordinates of particles). The channel occupies $0 < b < L/2$, where L is the fundamental wavelength in the a-direction.

The channel walls are rigid:

$$Y(a, 0, t) = 0; \qquad Y(a, L/2, t) = L/2. \tag{5.1}$$

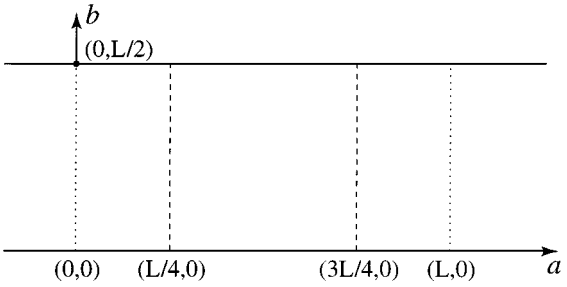

FIG. 2. Periodic channel; wavelength L in the long-channel Lagrangian Cartesian coordinate a; rigid boundaries at $b = 0, L/2$; inner section $L/4 \leq a \leq 3L/4$.

All fields are periodic in a:

$$h(L, b, t) = h(0, b, t), \tag{5.2a}$$

$$X(L, b, t) = X(0, b, t) + L \tag{5.2b}$$

$$Y(L, b, t) = Y(0, b, t). \tag{5.2c}$$

Any choices of initial conditions

$$\mathbf{X}(\mathbf{a}, 0) = \mathbf{a}, \qquad \mathbf{X}_t(\mathbf{a}, 0) = \mathbf{U}_I(\mathbf{a}), \qquad h(\mathbf{a}, 0) = h_I(\mathbf{a}) \tag{5.3}$$

that are compatible with (5.1) and (5.2) yield well-posed boundary-initial-value problems in the outer domain. For example, consider the following initial fields [13] in the absence of forcing

$$u_I(a, b) = U_0 - U_1 \sin\left(\frac{4\pi a}{L}\right) \cos\left(\frac{2\pi b}{L}\right) \tag{5.4a}$$

$$v_I(a, b) = 2U_1 \cos\left(\frac{4\pi a}{L}\right) \sin\left(\frac{2\pi b}{L}\right) \tag{5.4b}$$

$$h_I(a, b) = \frac{c^2}{g} + \left(\frac{L f U_1}{2\pi g}\right) \sin\left(\frac{4\pi a}{L}\right) \sin\left(\frac{2\pi b}{L}\right) + \left(\frac{U_1^2}{4g}\right) \left\{ \cos\left(\frac{8\pi a}{L}\right) + 4\cos\left(\frac{4\pi b}{L}\right) \right\} - \left(\frac{f U_0}{g}\right)\left(b - \frac{L}{2}\right), \tag{5.4c}$$

where c is a phase speed. These fields are initially "balanced" in the sense that at $t = 0$,

$$J_t = J_{tt} = 0. \tag{5.5}$$

It follows that the Eulerian flow divergence $\boldsymbol{\nabla}_x \cdot \mathbf{u}$ vanishes initially, as does its Eulerian local rate of change $\frac{\partial}{\partial t}(\boldsymbol{\nabla}_x \cdot \mathbf{u})$. The initial values (5.4) lead to smooth fields after an advective time scale $t = T = L/(2U_0)$: see, for example, the long-channel velocity $u \equiv X_t$ in Fig. 3. In brief, the numerics are second-order centered differences in space on the C-grid [14], forward–backward differencing in time, no filtering, and simple first-order extrapolatory computational boundary conditions as needed. None are needed for the periodic channel. Parameter values are given in Table 1. Computed values of X, Y, and h at $a = L/4, 3L/4$, for $0 \le b \le L/2$, and for $0 \le t \le T$ were used as boundary data for "nested"

TABLE 1

Parameter	Value
f	10^{-4} s^{-1}
L	2×10^4 m
U_0	0.5 m s^{-1}
U_1	0.1 m s^{-1}
c	2 m s^{-1} (subcritical flow)
	0.2 m s^{-1} (supercritical flow)
Δt	10 s
Δa (=Δb)	2×10^2 m

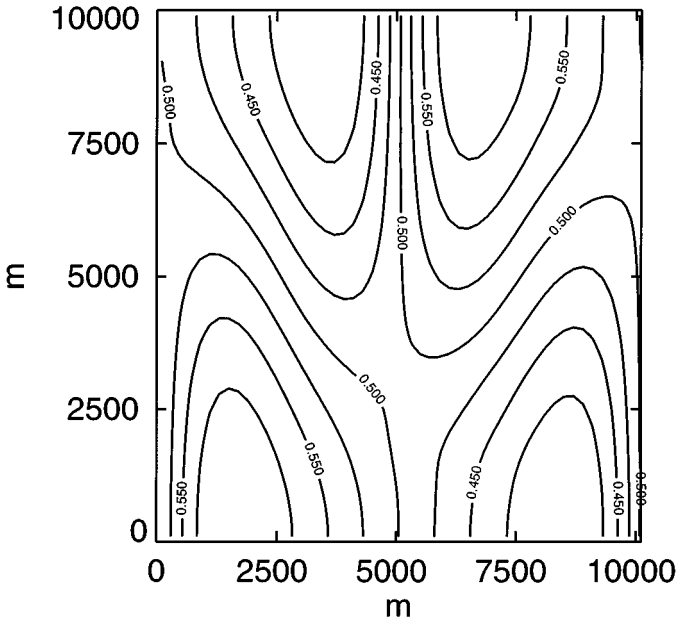

FIG. 3. The outer solution for the long-channel Lagrangian velocity $u = X_t$ at $t = T = L(2U_0)^{-1}$, in the inner domain $L/4 \le a \le 3L/4$, $0 \le b \le L/2$.

integrations in the channel section $L/4 \le a \le 3L/4$. Eight integrations will now be described, with the following variations:

(i) either subcritical ($U_0 < c$), or supercritical ($U_0 > c$) mean flow;

(ii) either two dynamical boundary conditions (DBCs) for X and h, and a computational boundary condition (CBC) for Y, at both $a = L/4$ and $a = 3L/4$, or three DBCs at both $a = L/4$ and $a = 3L/4$;

(iii) either "exact" numerical boundary data from the integration in the outer domain provided at $a = L/4$ and $a = 3L/4$, or "corrupted" data. The data were corrupted as

$$X(a, b, t_k) = \begin{cases} X(a, b, t_k), & 1 \le k \le 100 \\ r^k X(a, b, t_k), & 101 \le k \le 1000 \end{cases}, \tag{5.6}$$

where $t_k = k\Delta t$, $T = t_{1000}$ and $r = 0.99998$. Note that $r^{1000} = 0.98$ so the corruption is at most 2%.

For brevity, results from only some combinations will be displayed.

(a: subcritical flow, 2 DBCs, 1 CBC, exact data) The outer solution is recovered: see Fig. 4.

(b: subcritical flow, 3 DBCs, exact data) The outer solution is recovered: see Fig. 5.

(c: subcritical flow, 2 DBCs, 1 CBC, corrupted data) The outer solution is not recovered, but the result is a smooth field: see Fig. 6.

(d: subcritical flow, 3 DBCs, corrupted data) The result is not a smooth field: see Fig. 7. Integrating (d) beyond $t = T$ leads quickly to complete breakdown of the solution, as does integration from $t = 0$ to $t = T$ for $r = 0.99997$.

(e: supercritical flow, 2 DBCs, 1 CBC, corrupted data) The outer solution is not recovered, but the result is a smooth field: see Fig. 8.

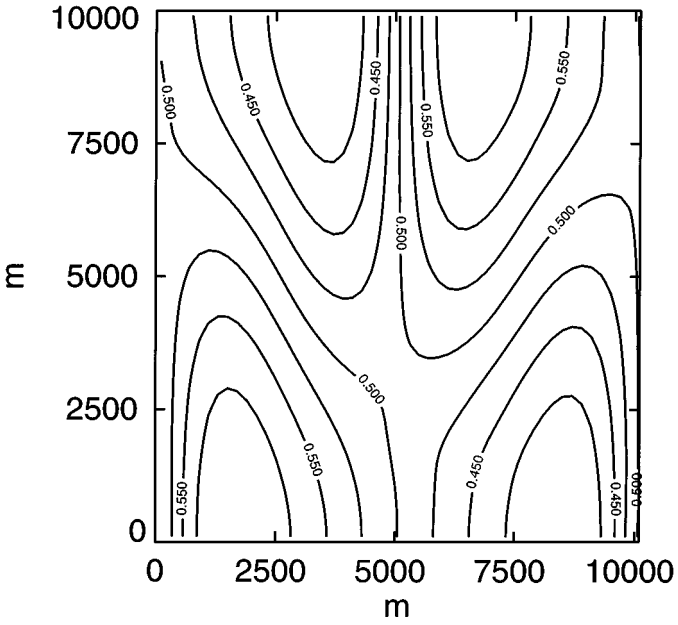

FIG. 4. Experiment (a): subcritical flow, two dynamical boundary conditions (DBCs), one computational boundary condition (CBC), exact boundary data from the outer solution. The outer solution is recovered.

(f: supercritical flow, 3 DBCs, corrupted data) The result is not a smooth field: see Fig. 9. Again integrations for longer time or greater corruption lead to solution breakdown.

In summary, these simple experiments support the theoretical arguments of Section 3 that h and $\mathbf{X} \cdot \hat{\mathbf{n}}$ may be specified on comoving boundaries, but not the tangential component of

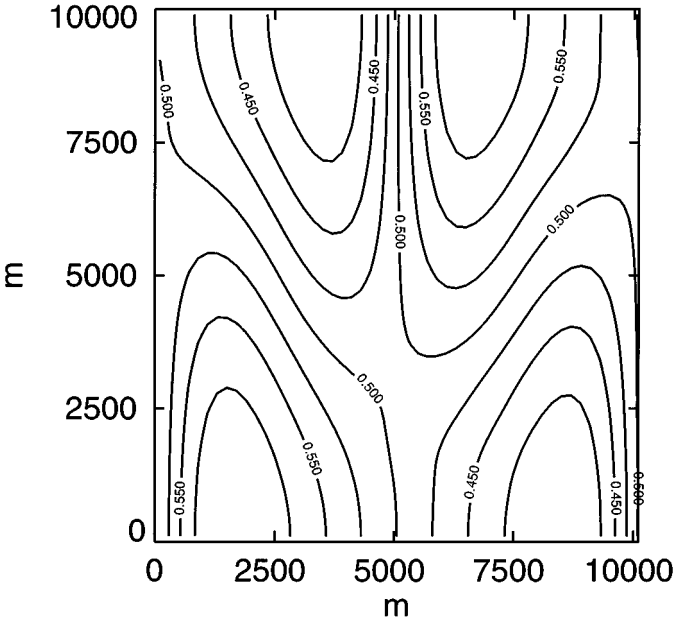

FIG. 5. Experiment (b): subcritical flow, three DBCs, exact data. The outer solution is recovered.

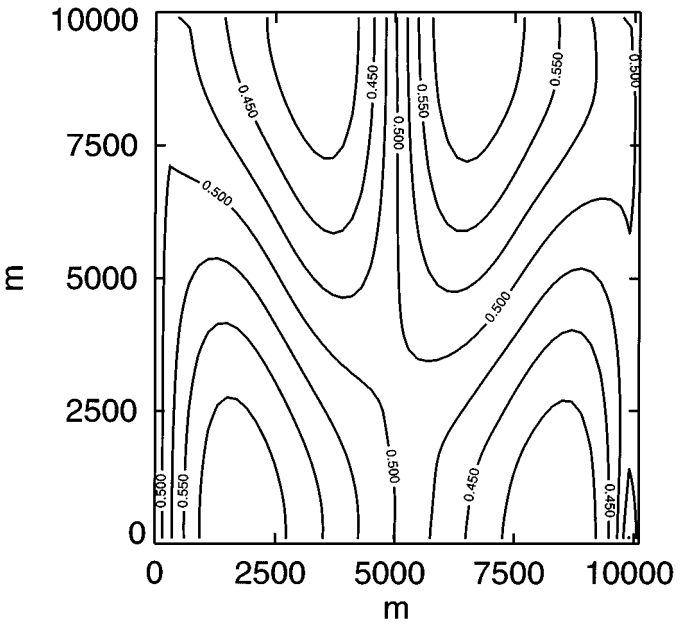

FIG. 6. Experiment (c): subcritical flow, two DBCs, one CBC, corrupted data. The inner solution differs from the outer, but is smooth.

X in addition. It is also clear that, of course, were the boundary data obtained from perfect observations of a real shallow-water flow (and filtered so as to be exactly consistent with a numerical model) or obtained from another consistent numerical computation, then the third or indeed even any number of dynamical boundary conditions could be prescribed. However,

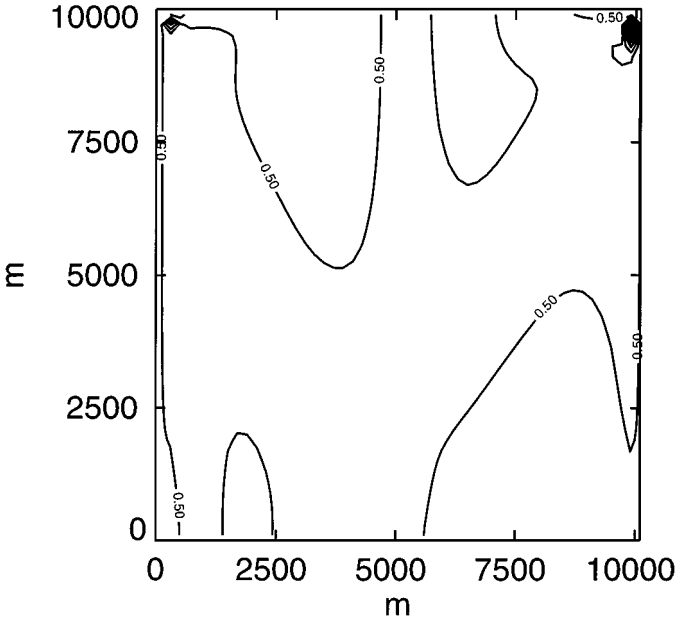

FIG. 7. Experiment (d): subcritical flow, three DBCs, corrupted data. The inner solution is not smooth.

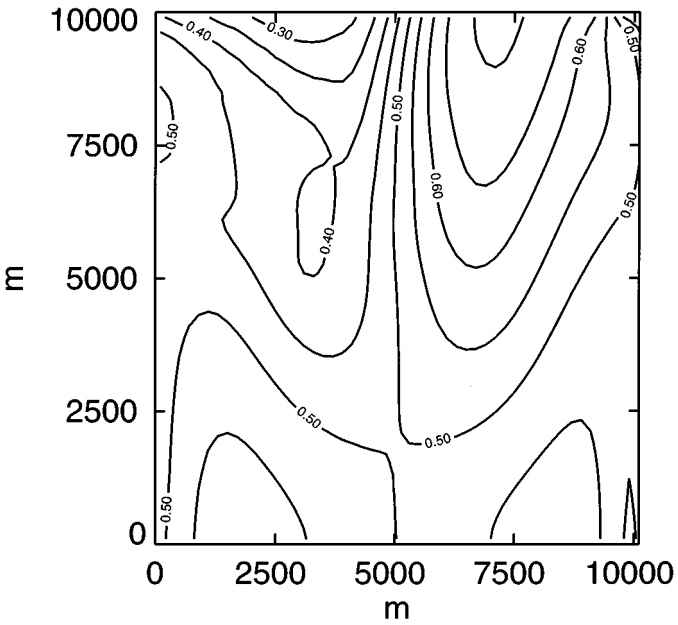

FIG. 8. Experiment (e): supercritical flow, two DBCs, one CBC, corrupted data. The inner solution differs from the outer (not shown), but is smooth.

the practical situation is that observations have significant errors and are inconsistently filtered, while numerical data derive from coarser outer numerical approximations.

It remains to demonstrate the efficiency of radiation conditions at comoving boundaries. Let $h^{(1)}$, $\mathbf{X}^{(1)}$ be the solution of problem (a) above, that is, the inner solution subject to the

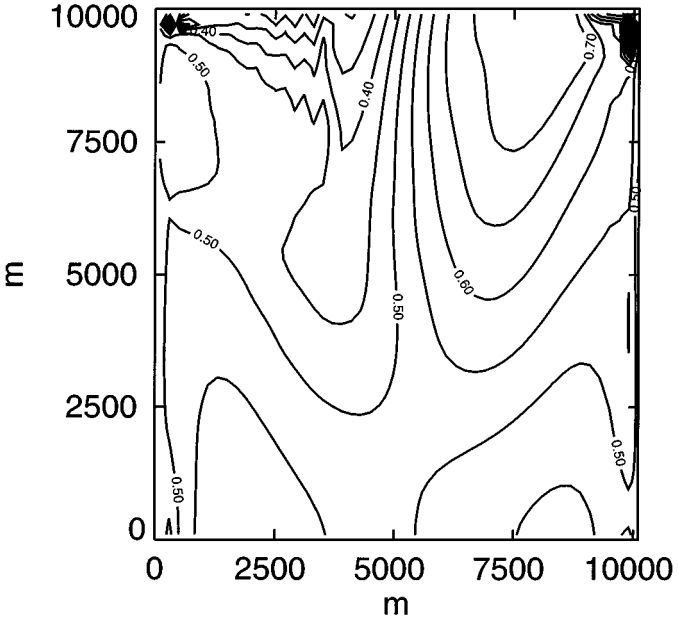

FIG. 9. Experiment (f): supercritical flow, three DBCs, corrupted data. The inner solution is not smooth.

initial values (5.4) and to boundary conditions on h and X, the boundary values h_{BC}, X_{BC} being uncorrupted values of the outer solution. Recall that $h^{(1)}$, $\mathbf{X}^{(1)}$ agree with the outer solution. Let $h^{(2)}$, $\mathbf{X}^{(2)}$ be the inner solution subject to the initial values (5.4) excepting that h_I is modified:

$$h_I^{(2)}(a,b) = h_I(a,b) \times \left\{1 + \epsilon \sin\left[\frac{\pi(a - L/4)}{L/2}\right] \exp[-((a - L/2)^2 + (b - L/4)^2)(L/2)^{-2}]\right\}. \tag{5.7}$$

Thus $h_I^{(2)}$ is modified by a bell-shaped "bump" of amplitude ϵ at $(L/2, L/4)$, which is tapered to vanish at $a = L/4, 3L/4$. Also $h^{(2)}$, $\mathbf{X}^{(2)}$ are subject to the linear, inhomogeneous radiation condition

$$X_t = X_{t_{BC}} \mp gc^{-1}(h - h_{BC}) \qquad \text{at } a = \begin{cases} L/4 \\ 3L/4 \end{cases} \tag{5.8}$$

plus the kinematic condition

$$X = X_{BC} \tag{5.9}$$

at $a = L/4, 3L/4$. That (5.8) and (5.9) together seem equivalent to the nonradiational conditions (3.21) is resolved by noting that the flow perturbations

$$\xi \equiv X^{(2)} - X^{(1)}, \qquad \chi = h^{(2)} - h^{(1)} \tag{5.10}$$

satisfy

$$\xi_t = \pm gc^{-1}\chi \tag{5.11}$$

at a boundary that has the total displacement (5.9). Long-channel sections of the perturbation χ on the centerline $b = L/4$ are plotted in Fig. 10 for $t = 0, T/2, T, 2T$. As expected, there is

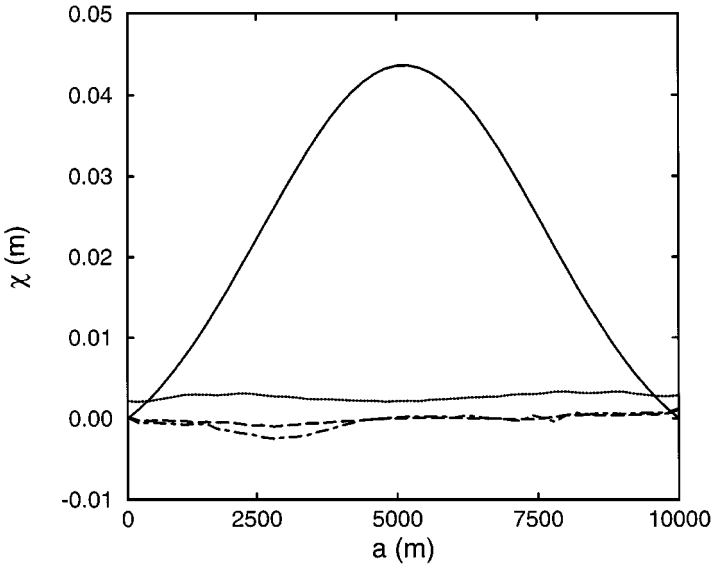

FIG. 10. Long-channel sections of height difference $\chi \equiv h^{(2)} - h^{(1)}$ at $0, T/2, T, 2T$; $b = L/4$, subcritical flow, initial bump amplitude $\epsilon = 0.1$. The disturbance smoothly exits the inner domain. Solid line: $t = 0$; dotted line: $t = T/2$; dashed line: $t = T$; dot-dashed line: $t = 2T$.

no evidence of ill-posedness. The disturbance amplitude decays in time. That is, $h^{(2)} \sim h^{(1)}$ as $t \to \infty$. The bump in the free surface has exited the inner domain, and the outer solution is recovered asymptotically.

6. SUMMARY

It has been argued theoretically, and by numerical demonstration, that the initial-boundary-value problem for the primitive equations is well-posed in open comoving domains. In the Lagrangian reference frame, all modes are effectively subcritical at the boundary (the local Froude number vanishes identically) and so each mode requires the same number of boundary conditions: one, such as surface elevation, to determine the incoming gravity-wave radiation, with another, such as normal velocity, to determine the subsequent motion of the boundary.

The horizontal Lagrangian reference frame depends upon depth, which dependence will in general lead to distortion of initially rectilinear three-dimensional open domains. However, this is a technical issue, as opposed to the fundamental issue of ill-posedness, and has received little attention owing to a lack of motivation. The demonstration here of well-posedness in comoving open domains provides that motivation.

The comoving domain is conveniently expressed in Lagrangian coordinates. Suppose further that data, such as surface elevation or isopycnal depth h, have been collected by freely drifting or Lagrangian buoys. If $\mathbf{x} = \mathbf{X}(\mathbf{a}, t)$ is the buoy trajectory, and $h_E = h_E(\mathbf{x}, t)$ is the Eulerian field of elevation, then the data are of the form

$$d(t) = h_E(\mathbf{X}(\mathbf{a}, t), t), \tag{6.1}$$

where $\mathbf{a}$ is the initial position of the buoy. Now (6.1) is a nonlinear measurement, which would greatly complicate least-squares variational data assimilation. The tangent linearization of (6.1) is readily derived, but its impact on any iterative search algorithm may well be complex. If, on the other hand, $h_L = h_L(\mathbf{a}, t)$ is the Lagrangian field of elevation, then the data are of the form

$$d(t) = h_L(\mathbf{a}, t), \tag{6.2}$$

which is a linear measurement, and so ideally suited to least-squares variational assimilation. (Data from moored or Eulerian buoys would correspond, of course, to nonlinear measurements in Lagrangian coordinates.)

Comoving domains and Lagrangian coordinates evidently offer significant advantages for regional modeling. Finally it may be noted that, as the cost of fixed moorings are becoming prohibitive, surface drifters and subsurface floats are increasingly the observing platforms of choice.

ACKNOWLEDGMENTS

AFB is supported by NASA (5198-PO-0016) and ONR (N00014-99-1-0040). BSC is supported by the UCAR Visiting Scientist Programs. The figures were drafted by David Reinert and the manuscript was typed by Florence Beyer.

REFERENCES

1. J. Oliger and A. Sundström, Theoretical and practical aspects of some initial boundary value problems in fluid dynamics, *SIAM J. Appl. Math*. **35**, 419 (1978).
2. E. N. Lorenz, *The Nature and Theory of the General Circulation of the Atmosphere* (World Meteorological Organization, Geneva, 1967).
3. A. Robert and E. Yakimew, Identification and elimination of an inflow boundary computational solution in limited area with integrations, *Atmos. Ocean* **24**, 369 (1986).
4. E. Yakimew and A. Robert, Validation experiments for a nested grid-point regional forecast model, *Atmos. Oceans* **28**, 467 (1990).
5. A. Staniforth, Regional modeling: A theoretical discussion, *Meteorol. Atmos. Phys.* **63**, 15 (1997).
6. J. Côté, S. Gravel, A. Méthot, A. Patoine, M. Loch, and A. Staniforth, The operational CMC-MRB global environmental multiscale (GEM) model. Part I. Design considerations and formulation, *Mon. Wea. Rev.* **126**, 1373 (1998).
7. A. Bennett, *Inverse Methods in Physical Oceanography* (Cambridge Univ. Press, Cambridge, UK, 1992).
8. G. J. Haltiner and R. T. Williams, *Numerical Prediction and Dynamical Meteorology* (Wiley, New York, 1980), 2nd ed.
9. R. H. Kraichnan, Lagrangian-history closure for turbulence, *Phys. Fluids* **8**, 575 (1965).
10. H. Lamb, *Hydrodynamics* (Cambridge Univ. Press, Cambridge, UK, 1932).
11. A. F. Bennett, Open boundary conditions for dispersive waves, *J. Atmos. Sci.* **33**, 176 (1982).
12. B. Engquist and A. Majda, Radiation boundary conditions for acoustic and elastic wave calculations, *Comm. Pure Appl. Math*. **32**, 313 (1979).
13. T. Elvius and A. Sundström, Computationally efficient schemes and boundary conditions for a fine-mesh barotropic model based on the shallow-water equations, *Tellus* **25**, 132 (1973).
14. F. Mesinger and A. Arakawa, *Numerical Methods Used in Atmospheric Models*, GARP Publication Series No. 14 (WMO/ICSU Joint Organizing Committee, Geneva, 1976).